Mater. Res. Soc. Symp. Proc. Vol. 1751 © 2015 Materials Research Society
DOI: 10.1557/opl.2015.143

Nanosize effect in Germanium Nanowire Growth with Binary Metal Alloys

Subhajit Biswas [1], Colm O'Regan[1], Michael A. Morris[1,2] and Justin D. Holmes[1,2]

[1]Materials Chemistry & Analysis Group, Department of Chemistry and the Tyndall National Institute, University College Cork, Cork, Ireland.
[2] Centre for Research on Adaptive Nanostructures and Nanodevices (CRANN), Trinity College Dublin, Dublin 2, Ireland.
*

ABSTRACT

This article describes feasible and improved ways towards enhanced nanowire growth kinetics by reducing the equilibrium solute concentration in the liquid collector phase in a vapor-liquid-solid (VLS) like growth model. Use of bi-metallic alloy seeds (Au_xAg_{1-x}) influences the germanium supersaturation for a faster nucleation and growth kinetics. Nanowire growth with ternary eutectic alloys shows Gibbs-Thompson effect with diameter dependent growth rate. In-situ transmission electron microscopy (TEM) annealing experiments directly confirms the role of equilibrium concentration in nanowire growth kinetics and was used to correlate the equilibrium content of metastable alloys with the growth kinetics of Ge nanowires. The shape and geometry of the heterogeneous interfaces between the liquid eutectic and solid Ge nanowires were found to vary as a function of nanowire diameter and eutectic alloy composition.

INTRODUCTION

A popular route for growing high aspect ratio one-dimensional (1D) nanostructures is to use a metallic growth promoter in a liquid state, typically gold, as catalytic seed via a VLS mechanism [1, 2]. According to classical crystal growth theory, in VLS growth, growth velocity (v) is proportional to $(\Delta\mu/kT)^2$, where T is the synthesis temperature and $\Delta\mu$ is a thermodynamic quantity called supersaturation, which is the chemical potential difference between adatoms of growth species in the vapor phase and the solid crystal phase [3]. Supersaturation ($\Delta\mu$) is the driving force in a layer-by-layer crystal growth process [4]. In reference to the classical nucleation theory for 2D-island formation, the nucleation rate and the lateral growth rate of islands combine to contribute to the normal growth rate of crystals which have a direct dependence on supersaturation [5]. Altering the supersaturation will readily influence the growth behavior of nanowires, favoring faster crystallization rates at high $\Delta\mu$ values. The composition of the liquid metal-semiconductor binary eutectic alloy (Au-Ge), governs the supersaturation, or driving force [3] and hence nanowire VLS-growth kinetics. A shift in the liquidus curve, *i.e.* the equilibrium composition of the eutectic alloy, alters the supersaturation of the catalyst seeds which subsequently influences the kinetics of nanowire growth [6, 7].

In the synthesis of Group 14 nanowires, via VLS growth, Au is the popular growth promoter due to its low eutectic melting temperature and the high solubility of Group 14 growth species in Au. A shift in the liquidus of Au-Ge (or Au-Si) binary alloy can be achieved by incorporating an external metal (foreign) element into the metal-semiconductor eutectic [8]. The noble metal Ag is readily miscible with Au and they do not form intermetallic compounds or go through a phase

change upon dissolution [9]. Both Au and Ag have a simple binary phase diagram with Ge, *i.e.* they do not form "metal-germanide" line compounds. Incorporation of one of these metals (Ag or Au) into the other can therefore be used to manipulate the equilibrium growth concentration (C_e) in the eutectic melt at a certain temperature.

In-situ electron microscopy experiments provide a feasible way to calculate equilibrium concentrations of Ge [10] at elevated temperatures in metastable eutectic alloys, permitting determination of Ge-liquidus curves for different sized nanoscale binary and ternary systems. The behavior of the triple phase boundary (TPB) at the nanowire-liquid metal interface provides an understanding of growth phenomenon at an atomic level [11-15]. For example, interfacial energies and capillary forces during steady-state nanowire growth determine the dynamics of the seed droplet at the tip of a nanowire [12, 16]. Position and shape of the droplet at a nanowire tip determines the facet dynamics and hence nominal crystal growth. In-situ observation of liquid-solid interfaces at nanowire growth temperatures provides the opportunity to correlate liquid-solid interfacial behavior to nanowire growth kinetics.

In this article, the application of Au-rich ($Au_{0.80}Ag_{0.20}$) colloidal alloy nanoparticles as growth promoters for manipulating the growth kinetics of Ge nanowires via a VLS mechanism is detailed. The nanoscale behavior associated with the growth of Ge nanowires from ternary eutectic (Au-Ag-Ge) alloys, assuming an equilibrium growth scenario, is explored via post-growth high temperature in-situ electron microscopy.

EXPERIMENT

In this study, dodecanethiol-stabilized phase pure Au and Au-rich ($Au_{0.80}Ag_{0.20}$) alloy nanoparticles were synthesized by co-reducing a mixture of chloroauric acid ($HAuCl_4$) and silver nitrate ($AgNO_3$) in a chloroform/water biphasic solution [17]. Nanoparticles between 2.5-3 nm in diameter were precipitated with ethanol and dispersed in toluene for further use. These small colloidal alloy nanoparticles were deposited onto silicon (001) substrates (with native oxide) and dried at 180 °C under vacuum. A liquid injection chemical vapor deposition (LICVD) technique, using toluene as the solvent phase, was adopted for growing the Ge nanowires on the surface of Si (001) substrates. Diphenylgermane (DPG) was used as the Ge source in the reactions and the nanoparticle concentration in each case was fixed at 40 μmole cm^{-3}. The concentration of DPG in toluene was fixed at 5 μmol ml^{-1}.

The one-dimensional Ge nanostructures were analyzed using a FEI quanta 650 scanning electron microscope (SEM) and a JEOL 2100 transmission electron microscope (TEM) operated at 200 kV equipped with an EDX detector (Oxford Instruments INCA energy system). The TEM heating experiments were performed on a JEOL 2100 TEM equipped with a Gatan 652 high-temperature sample holder.

To measure the length of nanowires dark filed scanning TEM was used. Nanowires were transferred on to a carbon coated copper grid (through dry transfer process) and only nanowires with catalyst tips were considered for length measurements.

RESULTS & DISCUSSION

As anticipated from the phase diagram, the effective growth of Ge nanowires was achieved from the phase pure gold nanoparticles and AuAg alloy nanoparticles seeds ($Au_{0.80}Ag_{0.20}$) after a 45 min growth time, as shown in the scanning electron microscopy (SEM) images in figures 1a and b and respectively. The Ge nanowire length was observed to increase with the introduction of Ag in the nanoparticle seeds. This phenomenon directly relates to the shift in the Ge liquidus phase boundary in the bulk phase diagram, towards lower Ge concentrations, upon incorporation of Ag in the Au-Ge eutectic system (Figure 1c). The participation of AuAg alloy growth seeds in nanowire growth is confirmed by the energy dispersive x-ray (EDX) mapping performed on the metal tip of the nanowires (inset in figure 1b). At a synthesis temperature of 455 °C, a reduction in the equilibrium solubility of Ge from approximately 37 to 23 at. % is likely with a 20 at. % induction of Ag in the bulk Au_xAg_{1-x} alloy seeds. TEM analysis (Figure 1d) of the Ge nanowires exhibited a bulk diamond cubic crystal structure (PDF 04-0545), with <111> being the dominant growth direction (90 % of the nanowires are in <111> growth direction). The monocrystalline nature of the Ge nanowires, with a 2-4 nm amorphous oxide coating was also confirmed by TEM.

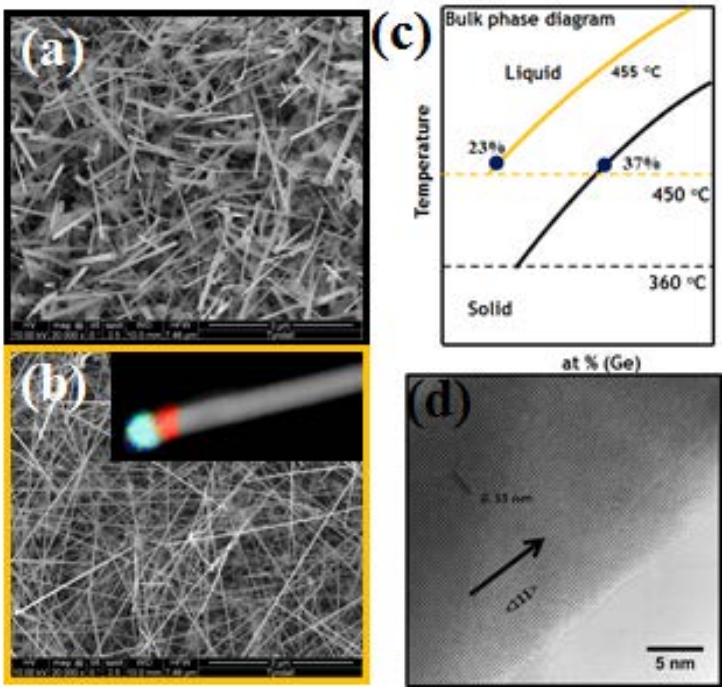

Figure 1. SEM images showing different lengths of nanowires observed with (a) Au seed and (b) $Au_{0.80}Ag_{0.20}$ alloy seeds and after 45 min of growth. Inset in (b) shows EDX map. Part (c) shows partial bulk phase diagram depicting the variation in equilibrium Ge concentration along the bulk Ge liquidus for two different catalyst – Ge growth systems . _Part (d) shows a TEM image of Ge nanowire with [111] growth direction.

A plot of nanowire growth rate distributions with two different seeds (see figure 2) clearly shows a fivefold increase in the nanowire growth rate with $Au_{0.80}Ag_{0.20}$ seeds compared to pure Au seeds. For a nanoscopic system having high surface-to-volume ratio the contribution of the surface energy to the thermodynamics is prominent, resulting in a diameter dependent growth rate [10]. Growth rate of Ge nanowires changes as a function of diameter, i.e. the participation of Gibbs-Thompson effect for the Au and alloy seeds and is shown in figure 2. A diameter dependent growth rate, obeying the Gibbs-Thompson rule, was observed for both the VLS-seeded nanowires; an increased growth velocity for larger diameter nanowires followed a quadratic dependence as formulated by Givargizov [3]. An increased nanowire growth rate (v) was also witnessed for the $Au_{0.80}Ag_{.020}$ -seeded Ge nanowires, compared to those synthesized from phase pure Au seeds, for the same diameter range. Increasing supersaturation with alloyed AuAg seeds lowers the thermodynamically achievable limit of the diameter for VLS-nanowire growth from 9.1 nm for Au seeded growth to 5.5 nm for $Au_{0.80}Ag_{0.20}$ alloy seeded growth at 455 °C as inferred from the

Gibbs-Thompson effect [6]. All of the arguments above are based on the assumption of a nucleation-mediated layer-by-layer growth mode obeying the Gibbs-Thompson effect. For nanowire growth near the eutectic temperature where simultaneous multiple nucleation events contribute together towards nanowire growth kinetics, the waiting time for Ge nucleation at the TPB is also influential chemical process. The enhanced supersaturation with AuAg alloy seeds increases the nucleation rate for each step and hence lowers the waiting time for an overall faster nanowire growth rate.

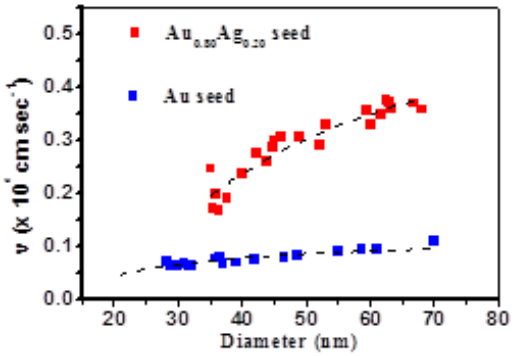

Figure 2. Plot show the quadratic dependence of the growth rate with nanowire diameter grown with different seeds.

The involvement of supersaturation-driven growth kinetics and the influence of equilibrium concentration was further observed by *in-situ* annealing experiments inside a TEM. The diameter dependent melting of metal seeds at the tips of Ge was observed in-situ. The change in the volume of Au-Ge and Au-Ag-Ge alloy liquid droplets as a function of temperature, for different diameter nanowires, was measured allowing the equilibrium compositions of Ge in the various eutectic melts to be determined [18]. The *in-situ* TEM heating experiments with different diameter nanowires for both the eutectic systems showed a direct demonstration of the size-dependent liquidus Ge concentration. Figures 3a and b show the evolution of nanowire shape with Au and $Au_{0.80}Ag_{0.20}$ droplets at the nanowire tips during the heat treatment from room temperature to 455 °C. Surface melting of eutectic droplets followed by melting of entire nanoparticles close to the respective bulk eutectic temperature (T_e) with an uptake of Ge from the nanowires was observed. Above the eutectic temperature the metal droplets at the tip become liquid. A further increase in temperature to 455 °C forces a gradual expansion in the liquid drop, due to an increase in the Ge content in the eutectic alloys. The diameter dependent Ge contents at 455 °C in eutectic alloys for different nanowire diameters are shown in figure 3c. The equilibrium Ge content decreased with an inclusion of Ag in the eutectic composition. Also, an upward trend in the Ge content as a function of decreasing nanowire diameter was evident for both eutectic systems. Thus lowering of the Ge equilibrium concentration at low temperatures in the eutectic regime can result in higher supersaturation and faster crystal growth as evident from figures 2 and 3. Discrepancy in experimental and theoretical plot could be due to the error in seed volume measurements. Though nanowire growth is mostly a non-equilibrium process (with varying transient concentration), growth

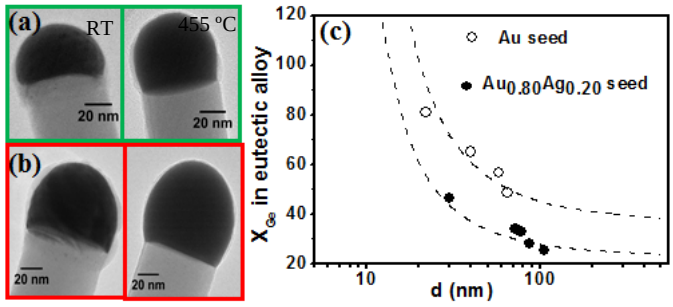

Figure 3. TEM images showing melting and expansion of metal seeds at the tip of Ge nanowire at 455 ºC upon Ge uptake for: (a) Au-Ge, (b) $Au_{0.80}Ag_{0.20}$-Ge. Part (c) shows Ge atomic % in the eutectic melt as a function of nanowire diameter for different alloy seeds.

kinetics can be interpreted in terms of equilibrium concentration as the difference in transient and equilibrium concentration determines the supersaturation.

The balance of interfacial forces (vapour-liquid (γ_{vl}), solid-liquid (γ_{sl}) and vapour-solid (γ_{vs}) surface energies) determines the equilibrium shape of the solid nanowire-liquid catalyst interface at steady state. However, recent theoretical and in-situ experimental studies have demonstrated a faceted interface at the TPB with truncation at the corner of the TPB contact lines [12-14]. The Young's balance of forces along the liquid-solid and vapor-solid interfaces account for stepped structures, *i.e.* facets, at the corner of the TPB contact line for <111> directed nanowires. The truncating facets mainly consist of the {113} family of planes at the corner of the TPB line. The schematic and TEM image of a AuGe liquid drop-Ge nanowire system (pictured at 420 ºC) and the SAED pattern recorded at the liquid-solid interface confirms the multi-faceted interface with central {111} planes surrounded by {113} faceted segments at the periphery (Figure 4a). Different liquid drop curvatures on nanowire sidewalls, *i.e.* different degrees of truncation of the contact line, were observed for the growth of varying diameter Ge nanowires from the Au-Ge eutectic system (Figure 4b). Equilibrium wetting angles (θ) at the tri-junction varied with the radial dimension of the nanowires. A pronounced wetting of the liquid drop, *i.e.* a decrease in the wetting angle (θ), into the nanowire sidewalls and a high degree of truncation of the TPB contact line was observed for thinner nanowires, whereas a much flatter growth front, with relatively small {113} facets at the corner of liquid-solid contact line was evident for thicker nanowires.

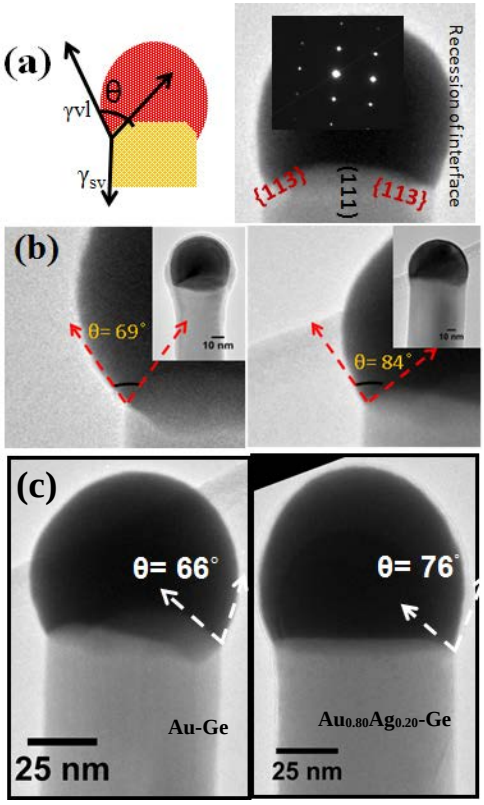

Figure 4. (a) Schematic and TEM image of a liquid drop-nanowire interface of Au-Ge eutectic and Ge nanowire with SAED pattern in the inset. Different wetting behavior is observed from TEM image of (b) Au-Ge eutectic and nanowire interface of different diameter and (c) Au-Ge and $Au_{0.80}Ag_{0.20}$-Ge eutectic with different wetting behavior.

Differences in the shape of the liquid-solid contact line are also observed with changes in the metal composition of the eutectics (Au and $Au_{0.80}Ag_{0.20}$) for similar diameter nanowires (d = 68 nm) in-situ annealed at the same temperature (Figure 4c). A large faceted growth front is observed with a pure Au-Ge system, whereas inclusion of Ag in the eutectic alloys forces the liquid-solid contact line towards a relatively flatter shape with smaller {113} corner facets. The greater amount of Ge present in the Au-Ge eutectic liquid alloy compared to the Au-Ag-Ge eutectic of similar size accounts for a smaller liquid surface energy (γ_{vl}) in Au-Ge compared in the Au-Ag-Ge alloys. For similar diameter nanowires, a greater imbalance in the Young's balance of forces at different interfaces with low γ_{vl} values for the Au-Ge system results in a faceted growth front, with higher facet curvature at the liquid-solid interface compared to Au-Ag-Ge system.

CONCLUSIONS

In summary, a new approach for controlling the growth behavior of Ge nanowires via a bottom-up VLS approach, employing AuAg alloy seeds, has been demonstrated. AuAg alloys facilitated the manipulation of thermodynamic growth limiting factors to produce favorable growth environments for longer nanowires and lowering of the limit of radial dimension in VLS nanowire growth, *i.e.* the *critical diameter*. The change in the equilibrium concentrations and supersaturation with different metal compositions in the alloys and different diameter nanowires was related to the different eutectic liquid-solid nanowire interfacial behavior.

ACKNOWLEDGMENTS

We acknowledge financial support from Science Foundation Ireland (Grant: 09/IN.1/I2602).

REFERENCES

1. S. Biswas, S. Kar and S. Chaudhuri, Journal of Physical Chemistry B **109** (37), 17526-17530 (2005).
2. G. Collins, M. Kolesnik, V. Krstic and J. D. Holmes, Chem. Mat. **22** (18), 5235-5243 (2010).
3. E. I. Givargizov, Journal of Crystal Growth **31** (DEC), 20-30 (1975).
4. B Lewis and J. S. Anderson, *Nucleation and Growth of Thin Films*. (Academic, New York, 1978).
5. D. T. J. Hurle, *Handbook of Crystal Growth*. (Elsevier, Amsterdam, 1994).
6. S. A. Dayeh and S. T. Picraux, Nano Lett. **10** (10), 4032-4039 (2010).
7. R. E. Algra, M. A. Verheijen, L. F. Feiner, G. G. W. Immink, W. J. P. van Enckevort, E. Vlieg and E. Bakkers, Nano Lett. **11** (3), 1259-1264 (2011).
8. P. L. A Prince, O Fabrichnaya, *Springer Materials The Landotl-Bornstein New Series IV/IIB*. (Springer, 2012).
9. S. Hassam, J. Agren, M. Gauneescard and J. P. Bros, Metallurgical Transactions a-Physical Metallurgy and Materials Science **21** (7), 1877-1884 (1990).
10. E. A. Sutter and P. W. Sutter, ACS Nano **4** (8), 4943-4947 (2010).
11. S. Hofmann, R. Sharma, C. T. Wirth, F. Cervantes-Sodi, C. Ducati, T. Kasama, R. E. Dunin-Borkowski, J. Drucker, P. Bennett and J. Robertson, Nature Materials **7** (5), 372-375 (2008).
12. A. D. Gamalski, C. Ducati and S. Hofmann, Journal of Physical Chemistry C **115** (11), 4413-4417 (2011).
13. C. Y. Wen, J. Tersoff, K. Hillerich, M. C. Reuter, J. H. Park, S. Kodambaka, E. A. Stach and F. M. Ross, Physical review letters **107** (2), 025503 (2011).
14. K. W. Schwarz and J. Tersoff, Nano Lett. **11** (2), 316-320 (2011).
15. V. G. Dubrovskii, G. E. Cirlin, N. V. Sibirev, F. Jabeen, J. C. Harmand and P. Werner, Nano Lett. **11** (3), 1247-1253 (2011).
16. K. W. Schwarz and J. Tersoff, Physical review letters **102** (20), 206101 (2009).
17. S. T. He, S. S. Xie, J. N. Yao, H. J. Gao and S. J. Pang, Applied Physics Letters **81** (1), 150-152 (2002).
18. E. Sutter and P. Sutter, Nano Lett. **8** (2), 411-414 (2008).